

Retraction

Retracted: Energy Efficiency Analysis in Modified GoF Spectrum Sensing-Based AF Relay Cooperative Cognitive Sensor Network with Energy Harvesting

Security and Communication Networks

Received 8 January 2024; Accepted 8 January 2024; Published 9 January 2024

Copyright © 2024 Security and Communication Networks. This is an open access article distributed under the Creative Commons Attribution License, which permits unrestricted use, distribution, and reproduction in any medium, provided the original work is properly cited.

This article has been retracted by Hindawi following an investigation undertaken by the publisher [1]. This investigation has uncovered evidence of one or more of the following indicators of systematic manipulation of the publication process:

- (1) Discrepancies in scope
- (2) Discrepancies in the description of the research reported
- (3) Discrepancies between the availability of data and the research described
- (4) Inappropriate citations
- (5) Incoherent, meaningless and/or irrelevant content included in the article
- (6) Manipulated or compromised peer review

The presence of these indicators undermines our confidence in the integrity of the article's content and we cannot, therefore, vouch for its reliability. Please note that this notice is intended solely to alert readers that the content of this article is unreliable. We have not investigated whether authors were aware of or involved in the systematic manipulation of the publication process.

Wiley and Hindawi regrets that the usual quality checks did not identify these issues before publication and have since put additional measures in place to safeguard research integrity.

We wish to credit our own Research Integrity and Research Publishing teams and anonymous and named external researchers and research integrity experts for contributing to this investigation.

The corresponding author, as the representative of all authors, has been given the opportunity to register their agreement or disagreement to this retraction. We have kept a record of any response received.

References

- [1] Y. Mi, G. Lu, and W. Gao, "Energy Efficiency Analysis in Modified GoF Spectrum Sensing-Based AF Relay Cooperative Cognitive Sensor Network with Energy Harvesting," *Security and Communication Networks*, vol. 2021, Article ID 3340525, 13 pages, 2021.

Research Article

Energy Efficiency Analysis in Modified GoF Spectrum Sensing-Based AF Relay Cooperative Cognitive Sensor Network with Energy Harvesting

Yin Mi ^{1,2}, Guangyue Lu ², and Wenbin Gao²

¹*Xi'an Institute of Optics and Precision Mechanics of CAS, University of Chinese Academy of Sciences, Xi'an 710119, China*

²*School of Communications and Information Engineering, Xi'an University of Posts and Telecommunications, Xi'an 710121, China*

Correspondence should be addressed to Guangyue Lu; tonylugy@163.com

Received 3 August 2021; Revised 17 September 2021; Accepted 3 November 2021; Published 30 November 2021

Academic Editor: Yinghui Ye

Copyright © 2021 Yin Mi et al. This is an open access article distributed under the Creative Commons Attribution License, which permits unrestricted use, distribution, and reproduction in any medium, provided the original work is properly cited.

In this paper, we propose a joint sensing duration and transmission power allocation scheme to maximize the energy efficiency (EE) of the secondary user (SU) in a cooperative cognitive sensor network (CSN). At the initial time slot of the frame, the secondary transmitter (ST) performs energy harvesting (EH) and spectrum sensing simultaneously using power splitting (PS) protocol. The modified goodness of fit (GoF) spectrum sensing algorithm is employed to detect the licensed spectrum, which is not sensitive to an inaccurate noise power estimate. Based on the imperfect sensing results, the ST will act as an amplify-and-forward (AF) relay and assist in transmission of the primary user (PU) or transmit its own data. The SU's EE maximization problem is constructed under the constraints of meeting energy causality, sensing reliability, and PU's quality of service (QoS) requirement. Since the SU's EE function is a nonconvex problem and difficult to solve, we transform the original problem into a tractable convex one with the aid of Dinkelbach's method and convex optimization technique by applying a nonlinear fractional programming. The closed-form expression of the ST's transmission power is also derived through Karush-Kuhn-Tucker (KKT) and gradient method. Simulation results show that our scheme is superior to the existing schemes.

1. Introduction

With the popularity of wireless devices in the Internet of Things (IoT) [1], it is expected to reach approximately 15.6 billion devices and connections by 2022. As a result, spectrum resources are becoming increasingly scarce. Motivated by this, cognitive radio (CR) technology is proposed and has attracted promising attention to cope with the spectrum utilization [2]. Generally, there are three models in CSN, including underlay, overlay, and interweave [3, 4]. In underlay CSN, the SUs can be allowed to coexist with the PU on the same frequency bands, but it is necessary to ensure that the interference to the primary receiver (PR) does not exceed the tolerance value, and therefore the SUs usually transmit information at a low transmission power to ensure the PU's QoS. In addition, the PU has the right to use the licensed spectrum for communication in interweave CSN, while the

SUs can only access to the spectrum holes opportunistically which are not occupied by the PU, and they need to detect the spectrum continuously during a period of time. Once the PU returns to the band, it is required for the SUs to evacuate immediately to avoid causing harmful interference to the PR [5]. And in overlay CSN, the ST acts as a relay to assist the PU's transmission through collaboration [6, 7]; in return, the ST can be allowed to access the licensed spectrum to transmit its own information. In this paper, we assume that the ST will act here as AF relay and assist the PU's transmission in the overlay CSN.

Meanwhile, it has been particularly noticed that the performance and reliability of wireless communication system are significantly limited by the battery life of energy-limited devices. Simultaneous wireless information and power transfer (SWIPT) has now been widely concerned and is considered a promising technique to solve the energy

shortage problem [8], as it can provide perpetual power through radio frequency (RF) EH without the need to recharge or replace the battery. It is well known that the RF signals radiated by surrounding transmitters are always available, so RF EH is more sustainable and flexible than solar and wind energy, and wireless sensor nodes can be allowed to convert the RF signals into energy for their own information transmission. Based on this, two actual receiver structures called time-switching (TS) and PS are proposed and studied in detail [9]. In a PS receiver, energy and information transmission are split into two power streams for EH and information processing, while the two processes are divided over the time slots in a TS receiver.

Recently, RF EH in CSN has become the object of extensive research [10–18]. In [10], a two-phase decoded-and-forward (DF) relay model was constructed by employing adaptive PS at the ST node; the outage probability and throughput were analysed. In [11], the ST employed the TS protocol to harvest energy and decode the PT's information; the secondary throughput was maximized by optimizing the energy harvesting time and the ST's relaying power. In [12], the SU's EE maximization problem was formulated under energy causality and the PU's QoS requirement constraint; a joint time and power allocation scheme was proposed in the overlay network. In [13], the SU accessed the PU's channel in a hybrid interweave/underlay mode using the time division multiple access (TDMA) technique to maximize the SU's throughput. In [14], asymptotic closed-form expressions for the spectrum efficiency (SE) and outage probability were derived at the constraints of the interference temperature and residual energy harvested from PT in an underlay network. Due to the broadcasting nature of wireless communication, the primary user emulation attack (PUEA) and the eavesdroppers may threaten network security and defeat the sensing performance; secrecy capacity and secrecy outage probability were analysed in [15–18].

However, the above researches did not consider the effects of the spectrum sensing results on the SE and EE in CSN. The cognitive base station collected all sensing results from SUs and then made a global decision, so that the SUs could decide whether to transmit or not [19, 20]; the sum secondary throughput maximization problem was formulated under the conditions of finite and infinite battery capacity. In [21], the subchannels were split into two sub-channel sets, one for spectrum sensing and the other for EH; they aimed to maximize the sum secondary throughput by jointly optimizing the sensing time, subchannel set, and SU's transmission power. In [22], the trade-off problem between EE and SE was discussed to determine the optimal sensing time, final decision threshold, and SU's transmission power, wherein the SUs were divided into two groups, which participated either in spectrum sensing and EH or in PU's transmission and EH. In [23], spectrum sensing and EH can be realized simultaneously by the ST through PS mode, and residual energy maximization problem based on linear and nonlinear EH models was explored under the constraints of sensing reliability and secondary and secrecy outage probability. In [24], the SU made the decision based on its location, the sensing result, and the battery's residual energy.

Moreover, a greedy policy of the SU was proposed and the optimal detection threshold was found to achieve the maximum throughput.

In an actual wireless communication, spectrum sensing may often be inaccurate. To the best of our knowledge, an imperfect spectrum sensing-based EE analysis has not yet been much investigated with EH in overlay CSN. Moreover, compared with ED and the original GoF algorithm, the modified GoF spectrum sensing algorithm can obtain better detection performance [25]. Since it is insensitive to variance under noise uncertainty, an inaccurate noise power estimate will not affect its detection performance. In addition, because the ranking operation is not required in the method, its computational complexity is significantly reduced, which is beneficial for energy-limited sensors in CSN.

Motivated by this, we propose a joint sensing time and power allocation scheme to maximize the SU's EE in the modified GoF spectrum sensing-based cooperative CSN with EH, where simultaneous EH and spectrum sensing are done at the ST node using PS mode and it can collaborate with PU's transmission using AF protocol. The major contributions of this paper are summarized as follows:

- (i) In spectrum sensing-based cooperative CSN with EH, the ST node employs the modified GoF algorithm to detect the PU's licensed spectrum. Based on the imperfect decision results, the ST either acts as AF relay and assists in PU's transmission or transmits its own data. We study the optimal sensing time and power allocation for maximizing the SU's EE under the constraints of meeting energy causality, sensing reliability, and PU's quality of service (QoS) requirement.
- (ii) By applying a nonlinear fractional programming method, we transform the original nonconvex EE problem into a tractable convex one with the aid of Dinkelbach's method and convex optimization technique. An iterative optimization algorithm is proposed for seeking the optimal sensing time and power allocation policy jointly. Meanwhile, the closed-form expression of ST's transmission power is also derived through KKT and gradient method.
- (iii) Simulations results verify the convergence of our proposed iterative scheme, and considering the linear and nonlinear EH model, we analyse the effect of the ST's maximal transmission power on the SU's EE when given different PU's QoS requirement. With the change of the sensing time and the power splitting ratio, the influence of an idle channel probability and given detection probability on the SU's EE is also analysed. Moreover, the EE curves are compared with the change of the noise uncertainty, verifying the superiority of the modified GoF algorithm.

The rest of this paper is organized as follows. In Section 2, the system model is formulated. The problem formulation and the proposed solution are introduced in Section 3. Finally, simulation results are provided in Section 4, and Section 5 concludes the paper.

2. System Model

As depicted in Figure 1(a), we consider a modified GoF spectrum sensing-based cooperative CSN with EH that the SU network and the PU network coexist in the same frequency band, where the network is composed of a PT-PR pair and a ST-SR pair. It is assumed that each node is working in half-duplex mode and is equipped with a single antenna. The ST can be regarded as IoT node, which has limited energy and computing power. In our model, simultaneous EH and spectrum sensing are done at the ST node using PS mode. Due to obstacles or deep fading, there is no direct communication link between PT and PR. To access the PU's licensed spectrum, the SU node must detect whether there is the PU signal or not in the frequency band. Herein, the ST employs the lightweight modified GoF algorithm for spectrum sensing. According to the decision results, the ST will either take part in relaying PU's transmission or transmit its own data. Let hypothesis 0 (H_0) denote that PU is inactive and the channel is idle and let hypothesis 1 (H_1) denote the presence of PU. The frequently used symbols in this paper are summarized in Table 1.

The instantaneous channel gains, between the PT and the ST link, the ST and the PR link, and the ST and the SR link, are denoted by h_{ps} , h_{sp} , and h_{ss} , respectively. Here, we assume that the links employ Rayleigh flat fading channel model in the cooperative CSN. Let d_{ij} be the distance from the i -th transmitter to the j -th receiver. Then, the instantaneous channel gain of the i - j link is denoted by $h_{ij} \sim \text{CN}(0, d_{ij}^{-\alpha})$ where α is the path loss exponent. Meanwhile, the CSI at the receivers are assumed to be available.

As illustrated in Figure 1(b), the entire frame duration T is divided into three distinct time slots repeating over a frame by frame transmission. Over the first time slot αT , the ST performs EH and spectrum sensing simultaneously using PS protocol, and the received signal power is split by the power splitting device with a ratio of θ : $(1-\theta)$ for EH and spectrum sensing, respectively. The modified GoF algorithm is used by the ST to detect the occupancy of the licensed spectrum; the PU is assumed to be either idle or active throughout the entire frame duration. In time slot $(1-\alpha)T/2$, the PT will transmit its own information to the ST. According to the decision result, the ST will decide to assist PU's transmission or transmit its own data during the remaining time slot $(1-\alpha)T/2$, where $0 < \alpha < 1$.

During the local spectrum sensing, the i -th ($i = 1, 2, \dots, n$) instantaneous sample of the received signal $y_{ST}(i)$ of the SU can be formulated as

$$y_{ST}(i) = \varphi \sqrt{\rho} h_{ps} x_p(i) + w_{ST}, \quad i = 1, 2, \dots, n, \quad (1)$$

where $x_p(i)$ is the transmitted signal by the PU with zero mean and variance $E[|x_p|^2] = P_T$, w_{ST} is assumed to be a circularly symmetric complex Gaussian (CSCG) random variable with zero mean and variance $E[|w_{ST}|^2] = P_{ns}$, and ρ is denoted by the signal-to-noise (SNR) $= 10 \lg(\rho |h_{ps}|^2 P_T / P_{ns})$. φ acts as a binary indicator; $\varphi = 1$ or 0 indicates the PU being active or idle, respectively. The ST node using PS protocol splits the received signal for spectrum sensing and

EH as $y_{ST1}(i) = (1-\theta)y_{ST}(i)$ and $y_{ST2}(i) = \theta y_{ST}(i)$, respectively. n represents the number of samples, i.e., $n = \alpha T f_s$, where f_s denotes the sampling frequency. Without loss of generality, we also assume that x_p and w_{ST} are independent of each other.

One part of the received signal at the ST is used for spectrum sensing. GoF tests measure the distance of the empirical cumulative distribution function (CDF) of the received samples and CDF in H_0 to detect the state of the PU. To be specific, let $F_n(y_{ST1})$ denote the empirical CDF of $y_{ST1}(i)$. In H_0 , $F_n(y_{ST1}) = F_0(y_{ST1})$ according to Glivenko-Cantelli theorem. Alternatively, H_1 is the hypothesis that $F_n(y_{ST1}) \neq F_0(y_{ST1})$. Therefore, spectrum sensing can be realized via the distance of $F_n(y_{ST1})$ and $F_0(y_{ST1})$. Here, the distance of $F_n(y_{ST1})$ and $F_0(y_{ST1})$ is defined as

$$W_n^2 = n \int_{-\infty}^{+\infty} [F_n(y_{ST1}) - F_0(y_{ST1})]^2 dF_0(y_{ST1}) = \sum_{j=1}^{\infty} \frac{z_{nj}^2}{j^2 \pi^2}, \quad (2)$$

where $z_{nj} = \sqrt{2/n} \sum_{i=1}^n \cos(j\pi F_0(y_{ST1}(i)))$.

W_n^2 is equal to the weighted sum squares of a set of test statistics z_{nj} ($j = 1, 2, \dots$). Besides, the different component is sensitive to different kinds of deviation, so that each measures some distinctive aspect of the sample distribution. For example, the first component z_{n1} is sensitive to mean shift but insensitive to variance shift. Based on this characteristic, the modified GoF method employs z_{n1} as the test statistic

$$z_{n1} = \sqrt{\frac{2}{n}} \sum_{i=1}^n \cos(\pi F_0(y_{ST1}(i))), \quad (3)$$

z_{n1} under H_0 follows normal distribution with zero mean and variance unit, and the PDF of z_{n1} is an even function. According to the central limit theorem, z_{n1} can be approximated under H_0 and H_1 . Consequently, the closed-form expression of the false alarm probability P_f is given as

$$P_f = \Pr\{z_{n1} \geq \gamma_r \text{ or } z_{n1} \leq \gamma_l | H_0\} \\ = 1 - Q(\gamma_r) + Q(\gamma_l) = 2Q(-\gamma), \quad (4)$$

where $Q(\cdot)$ is the complementary distribution function of the standard Gaussian; it can be given as follows:

$$Q(x) = \frac{1}{\sqrt{2\pi}} \int_x^{\infty} \exp\left(-\frac{t^2}{2}\right) dt. \quad (5)$$

Moreover, $\gamma_r = -\gamma_l = \gamma$. Then, the decision threshold for any P_f can be calculated by

$$\begin{cases} \gamma_r = Q^{-1}(P_f/2), \\ \gamma_l = -Q^{-1}(P_f/2). \end{cases} \quad (6)$$

According to (3), the test statistic z_{n1} can be calculated using the received signal samples $y_{ST1}(i)$. Through equation (6), we can get the decision thresholds γ_r and γ_l . Finally, the PU is absent if $z_{n1} > \gamma_l$ or $z_{n1} < \gamma_r$. Otherwise, reject H_0 in favour of the PU signal.

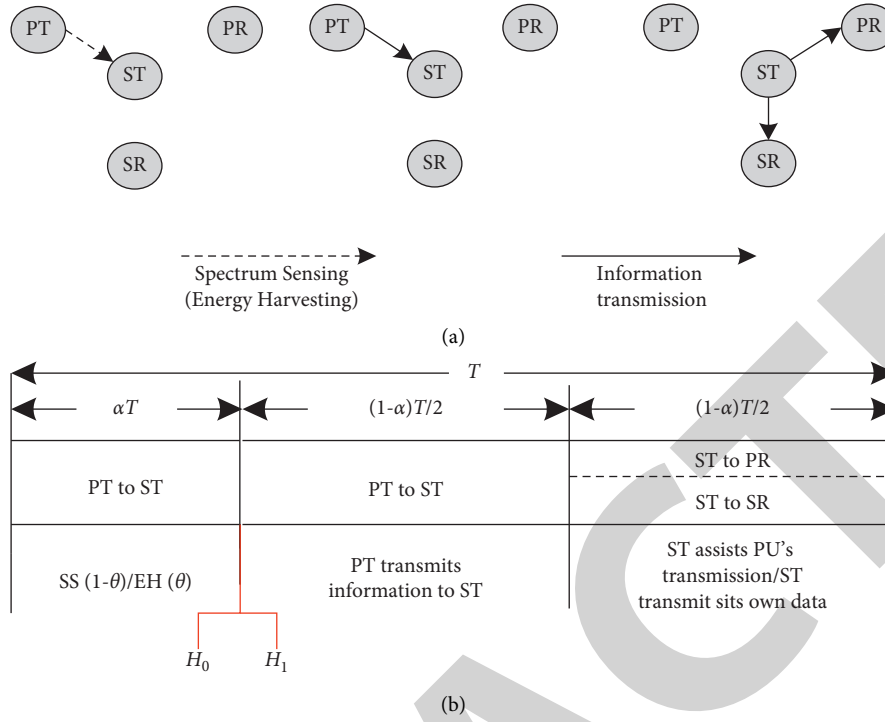


FIGURE 1: (a) System model. (b) Frame structure.

TABLE 1: List of symbols.

Symbols	Descriptions
T	Total frame duration
θ	Power splitting ratio
β	Amplifying power gain
ρ	Signal-to-noise (SNR)
p	Path loss exponent
φ	Binary indicator
η	Energy conversion efficiency
η_{EE}	Energy efficiency of SU network
f_s	Sampling frequency
N	Number of samples
H_0, H_1	PU is vacant and present
$P(H_0), P(H_1)$	Probability that the channel is idle and occupied
z_{n1}, z_{nj}	First component and a set of test statistics
$W(z)$	CDF of test statistic z_{n1}
W_n^2	Weighted sum squares of z_{nj}
$\gamma_r, \gamma_l, \gamma$	Decision threshold
y_{ST}	Instantaneous sample of the received signal
P_d	Given detection probability
R_{th}	PU's minimum throughput requirement
x_p, P_T	PU transmitted signal, PU transmission power
x_s, P_{SR}	ST transmitted signal, ST transmission power
E_h	Energy gathered at ST
P_s	Sensing power consumption
E_{tot}	Total energy consumption of SU
P_{max}	Maximal transmission power of ST
w_{PR}, P_{np}	Noise signal and variance at PU receiver
w_{ST}, P_{ns}	Noise signal and variance at the ST
w_{SS}, P_{nr}	Noise signal and variance at SU receiver
d_{ps}, d_{sp}, d_{ss}	Distance between PT and ST, ST and PR, and ST and SR
h_{ps}, h_{sp}, h_{ss}	Instantaneous channel gains between PT and ST, ST and PR, and ST and SR
R_p, R_{p1}, R_{p2}	PU's achievable throughput
R_s, R_{s1}, R_{s2}	SU's achievable throughput

Therefore, for a given P_f , the probability of detection P_d can be described as

$$P_d = \Pr\{z_{n1} \geq \gamma \text{ or } z_{n1} \leq -\gamma H_1\} = 1 - W(\gamma) + W(-\gamma), \quad (7)$$

and we can conclude that the CDF of test statistic z_{n1} , which follows $N(\mu_z, \sigma_z^2)$, can be described as

$$W(z) = \frac{1}{\sqrt{2\pi}\sigma_z} \exp\left(-\frac{(z - \mu_z)^2}{\sigma_z^2}\right), \quad (8)$$

where $\mu_z = \sqrt{2n} \int_{-\infty}^{+\infty} \cos(\sqrt{\pi}/\sqrt{2}\sigma \int_{-\infty}^{y_{ST1}(i)/(1-\theta)} e^{-x^2/2\sigma^2} dx) 1/\sqrt{2\pi}(1-\theta)\sigma e^{-(y_{ST1}(i)-(1-\theta)\sqrt{\rho}})^2/2(1-\theta)^2\sigma^2} dy_{ST1}(i)\sigma_z^2 = 2 \int_{-\infty}^{+\infty} [\cos(\sqrt{\pi}/\sqrt{2}\sigma \int_{-\infty}^{y_{ST1}(i)/(1-\theta)} e^{-x^2/2\sigma^2} dx)]^2 1/\sqrt{2\pi}(1-\theta) \sigma e^{-(y_{ST1}(i)-(1-\theta)\sqrt{\rho}})^2/2(1-\theta)^2\sigma^2} dy_{ST1}(i) - 2 \int_{-\infty}^{+\infty} \cos(\sqrt{\pi}/\sqrt{2}\sigma \int_{-\infty}^{y_{ST1}(i)/(1-\theta)} e^{-x^2/2\sigma^2} dx) 1/\sqrt{2\pi}(1-\theta)\sigma e^{-(y_{ST1}(i)-(1-\theta)\sqrt{\rho}/2(1-\theta)^2\sigma^2)} dy_{ST1}(i)]^2$.

It should be noted that the cooperative spectrum sensing is not considered in our work because only one ST performs spectrum sensing.

In the following, we introduce two EH models: including ideal linear EH model and practical nonlinear EH model. In the linear EH model, based on equation (1), the ST splits the received signal by the ratio θ for EH, so the energy gathered at the ST is expressed as

$$E_h^L = \eta\theta\alpha T \left(|h_{ps}|^2 P_T + P_{ns} \right), \quad (9)$$

where $0 \leq \eta \leq 1$ means the energy conversion ratio from the harvested energy into its battery; the received RF signals and noise by the ST node are used for energy harvesting during the spectrum sensing phase. We can note that, in the linear EH model, the energy conversion ratio η is independent of the input power P_T . But in the practical nonlinear EH model, the conversion efficiency is greatly relative to the input power level, the harvested power will saturate a constant value when the input power increases to a certain extent, and the sensitivity of the energy harvester is limited [26]. Hence, the amount of the harvested power by the ST is modeled as follows:

$$\Phi_h^{NL} = \frac{M/1 + \exp(-a(P_{ER} - b)) - M/1 + \exp(ab)}{1 - 1/1 + \exp(ab)}, \quad (10)$$

where Φ_h^{NL} is the logistic (or sigmoid) function with respect to the received RF power P_{ER} . M is a constant denoting the maximum harvested power at the ST when the EH circuit is saturated; a and b are utilized to capture the circuit characteristic. In practice, parameters M , a , and b can be easily obtained by a standard curve fitting tool [26]. In the nonlinear model, the harvested energy by the ST can be expressed as $E_h^{NL} = \Phi_h^{NL}\alpha T$; here Φ_h^{NL} is derived by setting P_{ER} to $\theta(|h_{ps}|^2 P_T + P_{ns})$. Regardless of the linear or nonlinear EH model, it is supposed that the ST's harvested energy is enough for the PU's relaying transmission and its own information transmission.

2.1. ST Cooperates with PU's Transmission. Because the PT-PR direct link is considerably weak compared to the PT-ST link and ST-PR link, we neglect the PT-PR link data transmission for simplicity. If the PU is considered to exist on the licensed frequency band through the detection of the ST node, it cooperates with PU's transmission in two equal subslots $(1-\alpha)T/2$. In the first subslot, the ST node will receive the signal from the PT and then employ AF protocol to amplify the received signal and forward it to the PR in the other subslot. Therefore, the received signal at the PR is shown below:

$$y_{PR} = \sqrt{\beta} h_{sp} y_{ST} + w_{PR}, \quad (11)$$

where β is an amplifying power gain and w_{PR} is modeled as CSCG noise at the PR with zero mean and variance $E[|w_{PR}|^2] = P_{np}$.

Here, we take into account the imperfect spectrum sensing in the sensing phase at the ST node, so there are two cases in which the ST node assists in PU's transmission. The first case denotes that the ST is able to detect correctly when the PU is present, and the PU's achievable throughput R_{p1} is expressed as

$$R_{p1} = \frac{(1-\alpha)T}{2} P(H_1) P_d \log_2 \left(1 + \frac{\beta |h_{sp}|^2 |h_{ps}|^2 P_T}{\beta |h_{sp}|^2 P_{ns} + P_{np}} \right). \quad (12)$$

In either case, the PU channel is actually idle but it is not detected correctly by the ST node; in the event of false alarm detection, the PU's achievable throughput R_{p2} is expressed as

$$R_{p2} = \frac{(1-\alpha)T}{2} P(H_0) P_f \log_2 \left(1 + \frac{\beta |h_{sp}|^2 |h_{ps}|^2 P_T}{P_{np}} \right), \quad (13)$$

where $P(H_0)$ is the probability that the channel is idle, while $P(H_1)$ is the probability that the channel is occupied. To sum up, the PU's corresponding achievable throughput during the $(1-\alpha)T/2$ slot is assumed to be $R_p = R_{p1} + R_{p2}$.

2.2. SU Transmits Its Own Information. When the PU is detected to be idle, the ST node will transmit its data to the SR node. The received signal at the SR from the ST during $(1-\alpha)T/2$ is shown below:

$$y_{SR} = h_{ss} x_s + w_{ss}, \quad (14)$$

and here, x_s is the ST transmitted signal with zero mean and variance $E[|x_s|^2] = P_{SR}$, which denotes the transmission power of the ST. The noise w_{ss} at the SR node is modeled as CSCG random variable with zero mean and variance $E[|w_{ss}|^2] = P_{nr}$. The SU's transmission in such situation occurs in two specific cases. In case that the PU channel is indeed idle and no false alarm appears, the SU's achievable throughput in the event of no false alarm R_{s1} is given as

$$R_{S1} = \frac{(1-\alpha)T}{2} P(H_0)(1-P_f) \log_2 \left(1 + \frac{|h_{ss}|^2 P_{SR}}{P_{nr}} \right). \quad (15)$$

In another case where the PU channel is actually active but it is not accurately detected, the primary transmission serves as interference to the SR node. The SU's achievable throughput in case of missed detection of the PU R_{S2} is given as

$$R_{S2} = \frac{(1-\alpha)T}{2} P(H_1)(1-P_d) \log_2 \left(1 + \frac{|h_{ss}|^2 P_{SR}}{|h_{ps}|^2 P_T + P_{nr}} \right). \quad (16)$$

Therefore, the SU's corresponding achievable throughput can be given as follows:

$$R_s = R_{s1} + R_{s2}. \quad (17)$$

In addition, the total energy consumption of the SU is expressed as

$$E_{tot} = (1-\theta)\alpha T P_S + \frac{(1-\alpha)T}{2} \kappa_1 \beta + \frac{(1-\alpha)T}{2} \kappa_2 P_{SR}, \quad (18)$$

where $\kappa_1 = P(H_0)P_f P_{ns} + P(H_1)P_d (d_{ps}^{-p} P_T + P_{ns})$, and $\kappa_2 = P(H_0)(1-P_f) + P(H_1)(1-P_d)$. The SU's total energy consumption is divided into three parts, the first part P_s represents the spectrum sensing power consumption of the ST, the second part $\kappa_1 \beta$ is the ST-assisted transmission power consumption when the PU is considered to exist, and the last part $\kappa_2 P_{SR}$ represents the ST's transmission power consumption when the PU is absent. It should be noted that energy consumption at the receiver is insignificant compared to the ST's transmission energy consumption, so we ignore this part of the energy consumption for simplicity [27]. Thus, the EE is defined as the ratio of the achievable throughput to the total energy consumption of the SU network, which is represented by

$$\eta_{EE} = \frac{R_s}{E_{tot}}. \quad (19)$$

3. Problem Formulation and Proposed Solution

Based on the above analysis, in an imperfect spectrum sensing-based cooperative CSN with EH, the SU's EE maximization problem is constructed under the constraints of meeting energy causality, sensing reliability, and PU's quality of service (QoS) requirement; the sensing time α and the transmission power P_{SR} are optimized jointly. The EE maximization problem can be formulated as the following fractional programming problem.

Problem P1:

$$\begin{aligned} \max_{0 \leq \alpha \leq 1, P_{SR}} \quad & \eta_{EE} = \frac{R_s}{E_{tot}}, \\ \text{s.t.} \quad & E_{tot} \leq E_h^L, \\ & R_p \geq R_{th}, \\ & P_d \geq \bar{P}_d, \\ & 0 \leq P_{SR} \leq P_{\max}, \end{aligned} \quad (20)$$

where (20) guarantees that the total energy consumed by the ST does not exceed the harvested energy from the PT; here we mainly focus on the linear EH model; the nonlinear EH model is similar. Equation (20) guarantees the PU's QoS constraint, where R_{th} is the PU's minimum throughput requirement. Generally speaking, the probability of false alarm P_f is much less than the detection probability P_d [28]. By approximation, we can conclude that $R_p \approx R_{p1}$; thus the amplifying power gain β can be calculated as

$$\beta = \frac{P_{np} \left(2^{2R_{th}/P} (H_1) P_d^{(1-\alpha)T} - 1 \right)}{|h_{sp}|^2 |h_{ps}|^2 P_T - \left(2^{2R_{th}/P} (H_1) P_d^{(1-\alpha)T} - 1 \right) |h_{sp}|^2 P_{ns}}. \quad (21)$$

In (20), \bar{P}_d is a given detection probability, which guarantees the reliability of detection performance. According to (7), the detection probability P_d decreases monotonically with the increase of the decision threshold γ , and hence the maximum EE can be obtained only when P_d acquires its lower bound \bar{P}_d . In (20), the transmission power P_{SR} is chosen subject to the transmit power limit; P_{\max} is the ST's maximal transmission power.

Unfortunately, due to the product of optimization variables in (20), the objective function is still nonconvex problem. To resolve this problem, we seek an optimal transmission power P_{SR} for a fixed value of sensing time α . Let the partial derivative of η_{EE} taken with respect to (w.r.t.) α be $\partial \eta_{EE} / \partial \alpha$, and we can conclude that $\lim_{\alpha \rightarrow 0} \partial \eta_{EE} / \partial \alpha = +\infty$ and $\lim_{\alpha \rightarrow 1} \partial \eta_{EE} / \partial \alpha < 0$, which declare there exists a stationary point that maximized η_{EE} . Since $\partial \eta_{EE} / \partial \alpha = 0$ is highly nonlinear, it is difficult to derive a closed-form expression of the optimal sensing time α^* .

Hence, the optimal sensing time α^* can be found using a one-dimensional exhaustive search method over the interval (0, 1). In the following, we focus on deriving the optimal value P_{SR}^* when α is fixed. Let q^* denote the maximum EE of the investigated system. Then, we have

$$q^* = \frac{R_s(\alpha^*, P_{SR}^*)}{E_{tot}(\alpha^*, P_{SR}^*)} = \max_{\alpha, P_{SR}} \frac{R_s(\alpha, P_{SR})}{E_{tot}(\alpha, P_{SR})} \quad (22)$$

where P_{SR}^* and α^* denote the optimal transmission power and sensing time, respectively.

To transform the problem into a tractable form, motivated by Dinkelbach's method, we translate the original objective function into a subtractive form by adapting a nonlinear fractional programming, such as

$F(\alpha, P_{SR}) = R_S(\alpha, P_{SR}) - qE_{tot}(\alpha, P_{SR})$. The transformation of the objective function can be summarized in Lemma 1.

Lemma 1. *The maximum EE q^* is achieved if and only if the following condition is satisfied:*

$$F(q^*) = \max_{\alpha, P_{SR}} R_S(\alpha, P_{SR}) - q^* E_{tot}(\alpha, P_{SR}) = R_S(\alpha^*, P_{SR}^*) - q^* E_{tot}(\alpha^*, P_{SR}^*) = 0. \quad (23)$$

Proof. please refer to [29] for the proof.

Then, based on Lemma 1, the original problem P1 can be rewritten as problem P2.

Problem P2:

$$\begin{aligned} \max_{P_{SR}} F(q) = & \frac{(1-\alpha)T}{2} \left[P(H_0)(1-P_f) \log_2 \left(1 + \frac{|h_{ss}|^2 P_{SR}}{P_{nr}} \right) \right. \\ & \left. + P(H_1)(1-P_d) \log_2 \left(1 + \frac{|h_{ss}|^2 P_{SR}}{|h_{ps}|^2 P_T + P_{nr}} \right) \right] \\ & - q \left[(1-\theta)\alpha T P_S + \frac{(1-\alpha)T}{2} \kappa_1 \beta + \frac{(1-\alpha)T}{2} \kappa_2 P_{SR} \right], \end{aligned} \quad (24)$$

where q is a nonnegative parameter. Note that the optimization problem P2 is convex w.r.t. P_{SR} , such that we can find the optimal power allocation using convex optimization

techniques. To resolve this convex optimization problem, the Lagrangian function of (24) can be expressed as

$$\begin{aligned} \mathcal{L}(P_{SR}, \alpha, \nu, \mu) = & \frac{(1-\alpha)T}{2} \left[P(H_0)(1-P_f) \log_2 \left(1 + \frac{|h_{ss}|^2 P_{SR}}{P_{nr}} \right) \right. \\ & \left. + P(H_1)(1-P_d) \log_2 \left(1 + \frac{|h_{ss}|^2 P_{SR}}{|h_{ps}|^2 P_T + P_{nr}} \right) \right] \\ & - q \left[(1-\theta)\alpha T P_S + \frac{(1-\alpha)T}{2} \kappa_1 \beta + \frac{(1-\alpha)T}{2} \kappa_2 P_{SR} \right] \\ & + \nu \left[\eta \theta \alpha T \left(|h_{ps}|^2 P_T + P_{ns} \right) - (1-\theta)\alpha T P_S - \frac{(1-\alpha)T}{2} \kappa_1 \beta - \frac{(1-\alpha)T}{2} \kappa_2 P_{SR} \right] \\ & + \mu \left[\frac{(1-\alpha)T}{2} P(H_1) P_d \log_2 \left(1 + \frac{\beta |h_{sp}|^2 |h_{ps}|^2 P_T}{\beta |h_{sp}|^2 P_{ns} + P_{np}} \right) - R_{th} \right], \end{aligned} \quad (25)$$

where ν and μ are nonnegative Lagrangian multipliers. By taking the derivative of (25) w.r.t. P_{SR} , the value of P_{SR} that maximizes $L(P_{SR}, \alpha, \nu, \mu)$ can be calculated from the KKT

condition $\partial \mathcal{L} / \partial P_{SR} = 0$; the transmission power P_{SR} can be achieved as follows:

$$P_{SR} = \left[\frac{1}{2} \left\{ \frac{1}{(q+\nu) \ln 2} - \frac{|h_{ps}|^2 P_T}{|h_{ss}|^2} + \sqrt{\left(\frac{|h_{ps}|^2 P_T}{|h_{ss}|^2} - \frac{1}{(q+\nu) \ln 2} \right)^2 + \frac{4m_1 |h_{ps}|^2 P_T}{m_2 |h_{ss}|^2}} \right\} \right]^+, \quad (26)$$

where $m_1 = P(H_0)(1 - P_f)$, $m_2 = (\nu + q)\kappa_2 \ln 2$.

After calculating the transmission power P_{SR} , the Lagrangian multipliers including ν and μ are associated with

$$\nu(t+1) = \left[\nu(t) - \varepsilon_1 \left(\eta\theta\alpha T \left(|h_{ps}|^2 P_T + P_{ns} \right) - (1-\theta)\alpha T P_S - \frac{(1-\alpha)T}{2} \kappa_1 \beta - \frac{(1-\alpha)T}{2} \kappa_2 P_{SR} \right) \right]^+, \quad (27)$$

$$\mu(t+1) = \left[\mu(t) - \varepsilon_2 \left(\frac{(1-\alpha)T}{2} P(H_1) P_d \log_2 \left(1 + \frac{\beta |h_{sp}|^2 |h_{ps}|^2 P_T}{\beta |h_{sp}|^2 P_{ns} + P_{np}} \right) - R_{th} \right) \right]^+, \quad (28)$$

where $[y]^+ = \max(0, y)$. Then, the transmission power P_{SR} can be recalculated based on the updated Lagrangian multipliers ν and μ ; the optimal transmission power can be found using this iterative process.

In summary, the overall procedures of the proposed scheme are described in Algorithm 1. Firstly, the initial values of the transmission power P_{SR} and the dual variable ν are given; then calculating the amplifying power gain β using equation (21), q is set to $R_S(\alpha, P_{SR})/E_{tot}(\alpha, P_{SR})$. Secondly, P_{SR} is calculated according to equation (26), and the dual variables, i.e., ν and μ , are updated iteratively according to equations (27) and (28) until the inner loop (from line 6 to line 9) converges. Finally, for the converged values, $R_S(\alpha, P_{SR})$ and $E_{tot}(\alpha, P_{SR})$, are updated, and the convergence of the outer loop (from line 4 to line 11) is checked. If the condition $|R_S(\alpha, P_{SR}) - q E_{tot}(\alpha, P_{SR})| < \varepsilon$ is satisfied, the algorithm can stop and P_{SR}^+ is returned. When α varies from 0 to 1, the optimal transmission power P_{SR}^* is found and the resulting EE are compared, enabling the optimal values to be found. \square

4. Simulation Results

In this section, the performance of the proposed scheme is illustrated via 10^4 Monte Carlo simulations through MATLAB. For the nonlinear EH model, we set $M = 0.024$ W, $a = 150$, and $b = 0.014$ according to the fitting results [26]. Numerical values of different system parameters are listed in Table 2. To verify the advantages of the proposed scheme, we investigate the effect of different parameters on the scheme's performance.

Figure 2 shows that the convergence of the SU's EE under different channel gains. In our considered cooperative CSN, we assume that the instantaneous channel gain h_{ss} employs Rayleigh flat fading channel model. Meanwhile, the CSI at the SR is assumed to be available, and our proposed scheme is independent of the channel fading. It can be observed that the convergence of the SU's EE can be achieved very well within five iterations, which illustrates the effectiveness of the proposed algorithm.

Figure 3 illustrates the variations of the SU's EE when the sensing time α varies under different PU's minimum throughput requirements R_{th} . It is seen that the SU's EE is a unimodal function of sensing time α ; the optimal EE value is noted at $\alpha^* = 0.55$ for $R_{th} = 0.2$. When less time is spent on spectrum sensing, the SU's throughput is small due to the high

equations (20b)–(20c) constraints, which can be updated by the gradient method.

false alarm probability P_f which reduces the SU's EE. As the sensing time α increases, the SU's EE value increases until the optimal sensing time α^* is reached. In addition, when α exceeds its optimal value, more power is required to assist PU's transmission to meet its minimum throughput requirement; thus the SU's EE will decline accordingly. Moreover, the optimal sensing time α^* gradually increases with the increase of R_{th} , which means that the ST node will take more time to collect energy and perform spectrum sensing.

In Figure 4, we compare the SU's EE of the two EH models when the ST's maximal transmission power P_{max} varies from 0 to 1W under different PU's minimum throughput requirements R_{th} ($R_{th} = 0.2, 0.5, 0.8$). It is interesting to note that as P_{max} increases, the SU's EE increases with the decrease of R_{th} . The reason is that high R_{th} requires the ST to be more likely to transmit sufficient power to satisfy throughput requirement, while more energy consumption of the ST node will lead to lower EE. In addition, we can also observe that the SU's EE increases rapidly when P_{max} is small; then it converges to its optimal value, which indicates that increasing P_{max} to a certain value can no longer improve the EE; on the contrary it causes a loss. As the power splitting ratio θ increases, the SU's EE will be improved because of harvesting more energy. Compared with the linear EH model, the EE's improvement adopting the nonlinear EH model is more obvious, because it can accurately reflect the nonlinear behaviors in the practical EH circuits.

Figure 5 shows the SU's EE curves of the two EH models as an idle channel probability $P(H_0)$ changes under different sensing time α ($\alpha = 0.3, 0.4, 0.5$). The PU's minimum throughput requirement $R_{th} = 0.2$. It is seen that the SU's EE curves are all unimodal functions of $P(H_0)$ values, and for different sensing time, $P(H_0)$ corresponding to the optimal value of SU's EE is increasing. For example, in Figure 5(a), the maximum value of SU's EE is taken in the case of $\alpha = 0.3$, $P(H_0) = 0.3$, and when $\alpha = 0.5$, the maximum value is obtained when $P(H_0) = 0.6$. It means that when α is limited, in order to achieve the optimal EE, the probability of the PU occupying the channel is as small as possible. However, when the PU's absence is severe, it will restrict the ST's energy harvesting, resulting in a decrease of SU's EE. From the nonlinear EH model in Figure 5(b), we can clearly see that the SU's EE improves significantly with the increase of the power splitting ratio θ .

- (1) for $\alpha = 0:1$
- (2) Initialize the transmission power P_{SR} , the maximum tolerance ε , EE q , a given detection probability $\overline{P_d}$ and Lagrangian multiplier ν
- (3) Calculate the amplifying power gain β using (21)
- (4) repeat
- (5) Set $q = R_s(\alpha, P_{SR})/E_{tot}(\alpha, P_{SR})$
- (6) repeat
- (7) Update the transmission power P_{SR} according to (26)
- (8) Update the Lagrange multipliers ν and μ according to equations (27) and (28)
- (9) until convergence of P_{SR}
- (10) Update $R_s(\alpha, P_{SR})$ and $E_{tot}(\alpha, P_{SR})$
- (11) until $|R_s(\alpha, P_{SR}) - qE_{tot}(\alpha, P_{SR})| < \varepsilon$
- (12) Return $P_{SR}^+ = P_{SR}$, $q^+ = q$
- (13) end for
- (14) $\alpha^* = \arg \max q^+$, $P_{SR}^* = P_{SR}^+$, $q^* = q^+$

ALGORITHM 1: Optimal sensing time and transmission power.

TABLE 2: List of simulation parameters.

Name	Value
Total frame duration T	1s
Path loss exponent p	4
Power splitting ratio θ	0.9
Energy conversion efficiency η	0.6
PU transmission power P_T	1 W
Sensing power consumption P_s	0.2 W
Noise variance at PU receiver P_{np}	0.001 W
Noise variance at SU receiver P_{nr}	0.001 W
Distance between PT and ST d_{ps}	1.5 m
Distance between ST and PR d_{sp}	2.5 m
Distance between ST and SR d_{ss}	2 m

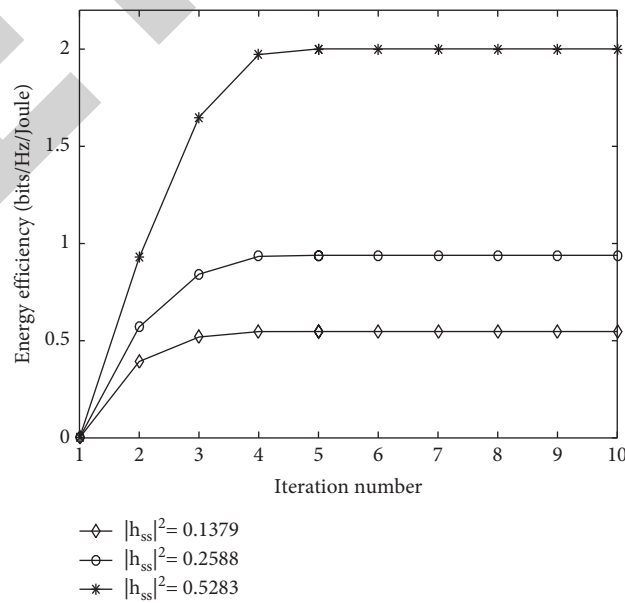
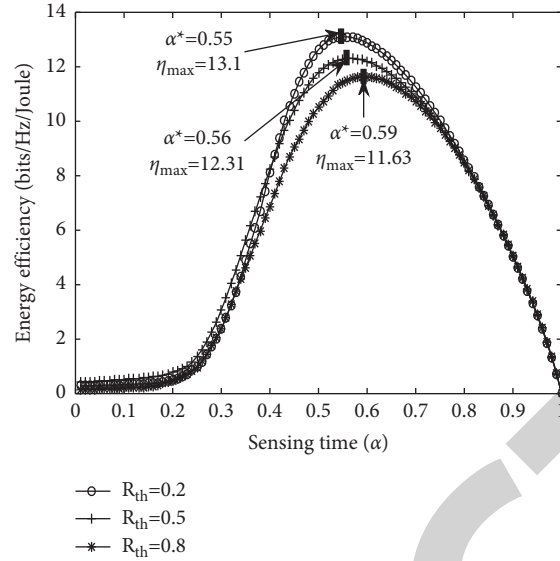
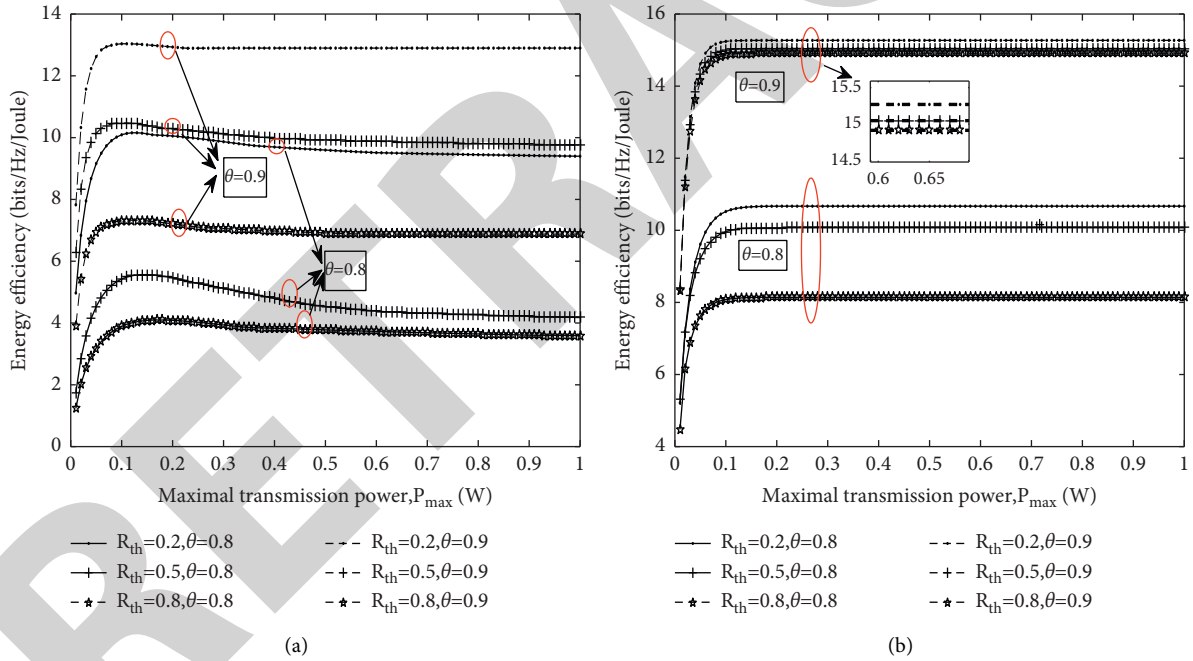


FIGURE 2: The SU's EE versus iteration number.

FIGURE 3: The SU's EE versus the sensing time α .FIGURE 4: The SU's EE versus $(P)_{\max}$. (a) Linear EH model. (b) Nonlinear EH model.

From Figure 6, it can be observed that the SU's EE decreases with the increase of a given detection probability \bar{P}_d when the sensing time α takes different values (0.3,0.4,0.5). For the same detection performance, the shorter the sensing time, the lower the SU's EE; the reason may be that the SU's energy consumption has increased accordingly. Similarly, the power splitting ratio θ is proportional to the SU's EE; it means that the ST node will harvest enough energy for the PU's assist transmission or its own data transmission.

In Figure 7, when the noise uncertainty varies from 0 dB to 3 dB, we compare the SU's EE of the modified GoF

algorithm, CM GoF, and ED algorithm. Because the modified GoF algorithm is insensitive to an inaccurate noise power, its false alarm probability P_f is constant and unchanging for different noise uncertainties (0 dB~3 dB), so the SU's EE curve is a straight line. While the SU's EE using the CM and ED algorithms are all decreasing slowly with the increase of the noise uncertainty, the false alarm probability of these two algorithms exceeds the given false alarm probability value, resulting in the decline of EE, which violates the requirements of the IEEE 802.22 standard.

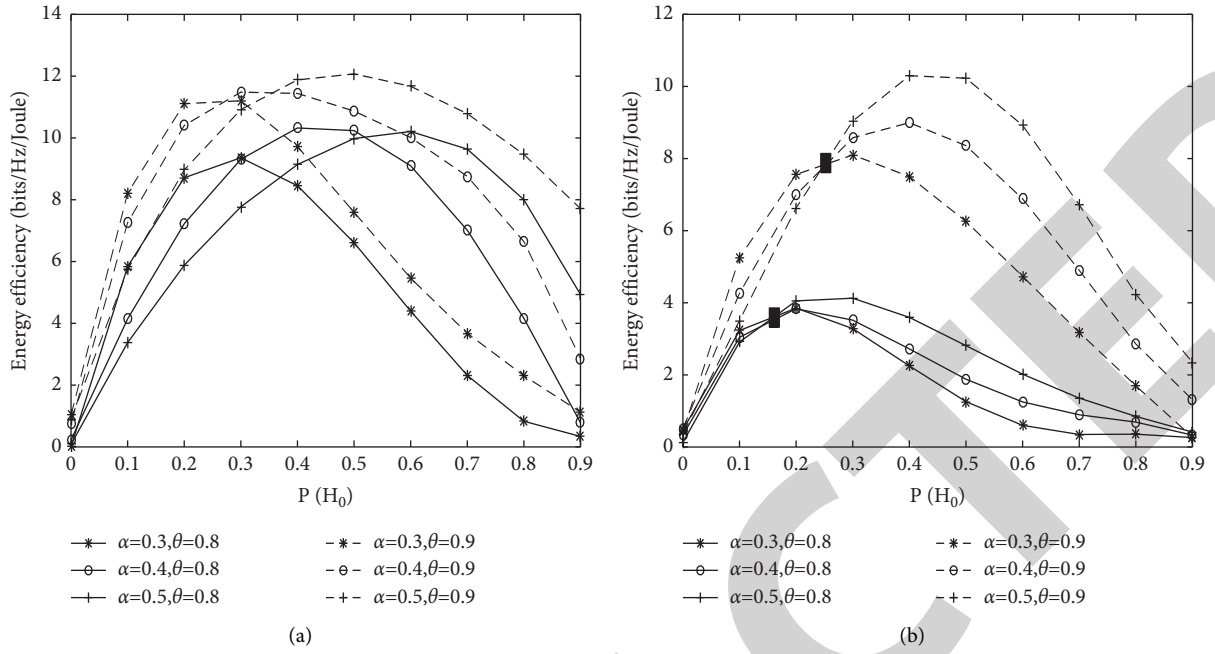


FIGURE 5: The SU's EE versus $P(H_0)$ ($P_{\max} = 1W$). (a) Linear EH model. (b) Nonlinear EH model.

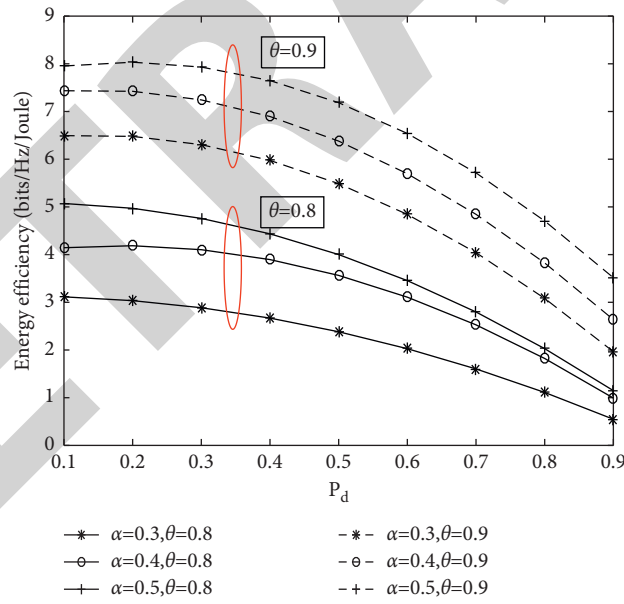


FIGURE 6: The SU's EE versus $\overline{P_d}$.

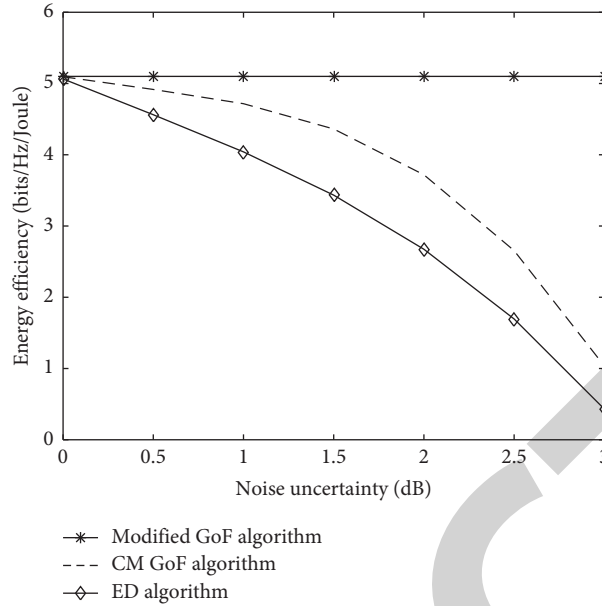


FIGURE 7: The SU's EE versus noise uncertainty.

5. Conclusions

In this paper, a joint sensing time and power allocation scheme is suggested to maximize the SU's EE in sensing-based cooperative CSN with EH under the constraints of meeting energy causality, sensing reliability, and PU's quality of service (QoS) requirement, where simultaneous EH and spectrum sensing can be done at the ST node using PS mode. The ST employs the modified GoF spectrum sensing algorithm to detect the spectrum usage, because of its ability to overcome noise uncertainty. Since the SU's EE maximization function is a nonconvex problem, we iterate for the optimal solutions by applying a nonlinear fractional programming, with the aid of Dinkelbach's method and convex optimization techniques. Simulation results show that the SU's EE can be improved with the decrease of R_{th} and is proportional to the power splitting ratio. Moreover, the SU's EE are all unimodal functions of α and $P(H_0)$. Finally, the SU's EE adopting different sensing algorithms are compared as the noise uncertainty changes, verifying the superiority of the modified GoF algorithm.

Data Availability

The data used to support the findings of this study are available from the corresponding author upon request.

Conflicts of Interest

The authors declare that there are no conflicts of interest regarding the publication of this paper.

Acknowledgments

This work was supported in part by the National Natural Science Foundation of China (Grant nos. 61701399 and 61801382) and the Science and Technology Innovation Team

of Shaanxi Province for Broadband Wireless and Application (Grant no. 2017KCT-30-02).

References

- [1] Q. Wu, G. Ding, Y. Xu et al., "Cognitive internet of things: a new paradigm beyond connection," *IEEE Internet of Things Journal*, vol. 1, no. 2, pp. 129–143, 2014.
- [2] J. Mitola III, "Cognitive radio for flexible mobile multimedia communications," *Mobile Networks and Applications*, vol. 6, no. 5, pp. 435–441, 2001.
- [3] B. Beibei Wang and K. J. R. Liu, "Advances in cognitive radio networks: a survey," *IEEE Journal of Selected Topics in Signal Processing*, vol. 5, no. 1, pp. 5–23, 2011.
- [4] Q. Qinyu Zhang, B. Bin Cao, Y. Ye Wang, A. Naitong Zhang, A. Xiaodong Lin, and A. Limin Sun, "On exploiting polarization for energy-harvesting enabled cooperative cognitive radio networking," *IEEE Wireless Communications*, vol. 20, no. 4, pp. 116–124, 2013.
- [5] Y. Mi, G. Lu, Y. Li, and Z. Bao, "A novel semi-soft decision scheme for cooperative spectrum sensing in cognitive radio networks," *Sensors*, vol. 19, no. 11, Article ID 2522, 2019.
- [6] Y. Chen, R. Shi, and W. Feng, "AF relaying with energy harvesting source and relay," *IEEE Transactions on Vehicular Technology*, vol. 66, no. 1, pp. 874–879, 2017.
- [7] X. Zhou and Q. Li, "Energy efficiency for SWIPT in MIMO two-way amplify-and-forward relay networks," *IEEE Transactions on Vehicular Technology*, vol. 67, no. 6, pp. 4910–4924, 2018.
- [8] X. Zhou, R. Zhang, and C. K. Ho, "Wireless information and power transfer: architecture design and rate-energy tradeoff," *IEEE Transactions on Communications*, vol. 61, no. 11, pp. 4754–4767, 2013.
- [9] R. Zhang and C. K. Ho, "MIMO broadcasting for simultaneous wireless information and power transfer," *IEEE Transactions on Wireless Communications*, vol. 12, no. 5, pp. 1989–2001, 2013.
- [10] Q. Li, X. Zhang, A. Pandharipande, and J. Zhang, "Cooperative spectrum sharing on SWIPT-based DF relay: an energy-

- aware retransmission approach,” *IEEE Access*, vol. 7, pp. 120802–120816, 2019.
- [11] F. Li, H. Jiang, and R. Fan, “Optimal cooperative strategy in energy harvesting cognitive radio networks,” in *Proceedings of the 86th Vehicular Technology Conference (VTC-Fall)*, pp. 1–6, IEEE, Toronto, Canada, September 2017.
- [12] F. Yan, J. Zhao, H. Qu, and X. Xu, “Energy-efficient cooperative strategy in RF energy harvesting cognitive radio network,” *Chinese Journal of Electronics*, vol. 28, no. 3, pp. 651–657, 2019.
- [13] A. F. Tayel, S. I. Rabia, A. H. A. El-Malek, and A. M. Abdelrazek, “An optimal policy for hybrid channel access in cognitive radio networks with energy harvesting,” *IEEE Transactions on Vehicular Technology*, vol. 69, no. 10, pp. 11253–11265, 2020.
- [14] Y. Liu, S. A. Mousavifar, Y. Deng, C. Leung, and M. ElKashlan, “Wireless energy harvesting in a cognitive relay network,” *IEEE Transactions on Wireless Communications*, vol. 15, no. 4, pp. 2498–2508, 2016.
- [15] P. Yan, Y. Zou, and J. Zhu, “Energy-aware multiuser scheduling for physical-layer security in energy-harvesting underlay cognitive radio systems,” *IEEE Transactions on Vehicular Technology*, vol. 67, no. 3, pp. 2084–2096, 2018.
- [16] L. Ni, X. Da, H. Hu, M. Zhang, and K. Cumanan, “Outage constrained robust secrecy energy efficiency maximization for EH cognitive radio networks,” *IEEE Wireless Communications Letters*, vol. 9, no. 3, pp. 363–366, 2020.
- [17] D. Wang and S. Men, “Secure energy efficiency for NOMA based cognitive radio networks with nonlinear energy harvesting,” *IEEE Access*, vol. 6, pp. 62707–62716, 2018.
- [18] M. Zhang, K. Cumanan, J. Thiyagalingam et al., “Energy efficiency optimization for secure transmission in MISO cognitive radio network with energy harvesting,” *IEEE Access*, vol. 7, pp. 126234–126252, 2019.
- [19] S. Biswas, S. Dey, and A. Shirazinia, “Sum throughput maximization in a cognitive multiple access channel with cooperative spectrum sensing and energy harvesting,” *IEEE Transactions on Cognitive Communications and Networking*, vol. 5, no. 2, pp. 382–399, 2019.
- [20] A. Banerjee and S. P. Maity, “On residual energy maximization in DF cognitive radio networks with multiple eavesdroppers,” *IEEE Transactions on Cognitive Communications and Networking*, vol. 6, no. 2, pp. 718–727, 2020.
- [21] X. Liu, F. Li, and Z. Na, “Optimal resource allocation in simultaneous cooperative spectrum sensing and energy harvesting for multichannel cognitive radio,” *IEEE Access*, vol. 5, pp. 3801–3812, 2017.
- [22] S. Chatterjee, S. P. Maity, and T. Acharya, “Energy-spectrum efficiency trade-off in energy harvesting cooperative cognitive radio networks,” *IEEE Transactions on Cognitive Communications and Networking*, vol. 5, no. 2, pp. 295–303, 2019.
- [23] A. Banerjee and S. P. Maity, “On residual energy maximization in cognitive relay networks with eavesdropping,” *IEEE Systems Journal*, vol. 13, no. 4, pp. 3836–3846, 2019.
- [24] K. Zheng, X. Liu, Y. Zhu, K. Chi, and Y. Li, “Impact of battery charging on spectrum sensing of CRN with energy harvesting,” *IEEE Transactions on Vehicular Technology*, vol. 69, no. 7, pp. 7545–7557, 2020.
- [25] Y. Mi and G. Lu, “Performance analysis of decomposed cramer-von mises detector for blind spectrum sensing under noise uncertainty,” in *Proceedings of the 10th International Conference on Wireless Communications and Signal Processing (WCSP 2018)*, pp. 1–6, IEEE, Hangzhou, China, September 2018.
- [26] H.-V. Tran, G. Kaddoum, and K. T. Truong, “Resource allocation in SWIPT networks under a nonlinear energy harvesting model: power efficiency, user fairness, and channel nonreciprocity,” *IEEE Transactions on Vehicular Technology*, vol. 67, no. 9, pp. 8466–8480, 2018.
- [27] T. T. Tran, D. H. N. Nguyen, T. Do-Hong, and S. Ngo-Van, “Achievable rates with cooperative spectrum sharing in the modulation-based dimension,” *IEEE Transactions on Vehicular Technology*, vol. 68, no. 1, pp. 654–670, 2019.
- [28] C. Stevenson, G. Chouinard, Z. Zhongding Lei, H. Wendong, S. Shellhammer, and W. Caldwell, “Ieee 802.22: the first cognitive radio wireless regional area network standard,” *IEEE Communications Magazine*, vol. 47, no. 1, pp. 130–138, 2009.
- [29] S. Boyd and L. Vandenberghe, *Convex Optimization*, Cambridge University Press, Cambridge, U.K., 2004.